2015 15th International Conference on Control, Automation and Systems (ICCAS 2015)
Oct. 13-16, 2015 in BEXCO, Busan, Korea

Advanced Control Strategy for Electric Power Steering System to Improve Steering Assist Torque Stability

Seunghwan Chung[1,2], Hyeongcheol Lee[3*]

[1] Department of Electrical Engineering, Hanyang University,
Seoul, 133-791, Korea (is95@hanyang.ac.kr)
[2] Vehicle Safety R&D Center, Korea Automotive Technology Institute,
Cheonan, 330-912, Korea (shchung@katech.re.kr)
[3] Division of Electrical and Biomedical Engineering, Hanyang University,
Seoul, 133-791, Korea (hclee@hanyang.ac.kr) * Corresponding author

Abstract: The EPS (electric power steering) system has been used to replace the conventional HPS (hydraulic power steering) system in vehicles. This system assists the steering effort of the driver using an electric motor and a gear force reduction. In a previous study, an EPS control method was proposed that used the driver's steering input torque and vehicle velocity. In addition, many papers have introduced estimation and control methods for the EPS motor's angular velocity or angular torque to reduce the sense difference for the HPS. Therefore, this paper proposes an advanced control strategy for EPS that uses the lateral force of the front wheels. In addition, we experimented with this proposed control algorithm using a simulation and confirmed that it reduced the assist torque and saved motor power. Although it is difficult to obtain the lateral wheel force of the tires for the proposed method, it is able to reduce the torque ripple of the EPS actuator, as well as troublesome problems with steering wheel vibration. Moreover, this EPS control strategy can improve a vehicle's dynamic stability.

Keywords: Electric power steering, Motor driven power steering, Electric power assisted steering, Steering torque control, Torque control stability, Torque ripple reduction

1. INTRODUCTION

In modern vehicles, traditional hydraulic power assist steering has been replaced by EPS (electric power steering) because of the improved fuel economy from the weight reduction [1-3]. EPS is able to provide variable assist torque only when it is needed such as during high-velocity driving and in parking mode by tuning its assist variable torque map. In addition, the fundamental control algorithm for EPS involves the determination of the assist motor current based on the driver's steering torque and vehicle velocity. For example, during a high-velocity period, this system should provide less assist torque to generate a solid steering feeling to improve driving stability. In contrast, for low-velocity maneuvers, it should provide more assist torque to generate a soft steering feel to improve driving maneuverability [4]. Many researchers have developed torque control methods for the EPS system based on alignment torque estimation [5-8]. These papers introduced methods to improve the vehicle driving stability and driver's steering feel by reforming the steering return torque. However, these studies failed to consider the alignment torque's nonlinear range, which is always a limit when trying to improve the steering assist torque stability. There have been other efforts to reduce the torque ripples of the EPS motor [9, 10]. However, these studies proposed methods to reduce the torque ripple by applying the estimated rotor position. In other words, the vehicle's driving condition was not considered, particularly the lateral friction force of the vehicle's tires. An EPS on-center handling improvement study introduced the use of a TAS (torque angle sensor), lateral acceleration sensor, and yaw rate sensor. However, the return ability control, damping compensation, inertia compensation, and tuning of numerous variable parameters in this method are very complicated [11, 12]. Therefore, this paper proposes an effective control strategy for the EPS assist torque stability, which is based on the lateral forces of the front wheels. This control strategy can reduce the assist steering torque ripple and reduce the BLDC (brushless DC) or BLAC motor current. The effectiveness and performance of the proposed EPS control concepts are verified in a DLC (double lane change) test mode using lumped mass vehicle dynamics modeling in a simulation environment. In addition, the same performance with less steering assist torque can be confirmed compared to the conventional EPS assist torque level in relation to the vehicle velocity and driver steering input.

2. EPS CONTROL CONCEPTS

2.1 EPS System Configurations

As shown in Fig. 1, EPS systems can be classified into four types depending on where the assist mechanism is located: column EPS, pinion EPS, dual pinion EPS, and rack EPS. As shown in Fig. 2, the EPS system types depend on the steering rack force [13]. In the column EPS system, the motor and ECU (electronic control unit) are mounted inside the cabin. Thus, no waterproofing is required, and there is no effect on engine room. Rack EPS has good steering performance from an accessibility advantage between the steering wheel and rack, and pinion EPS increases the load on the rack, pinion, and reduction gear. It is generally used in high-power applications. Therefore, the specific EPS system applied to a vehicle depends on the assist torque

level and vehicle size. This paper presents the column EPS system, which is widely applied to mass-produced vehicles.

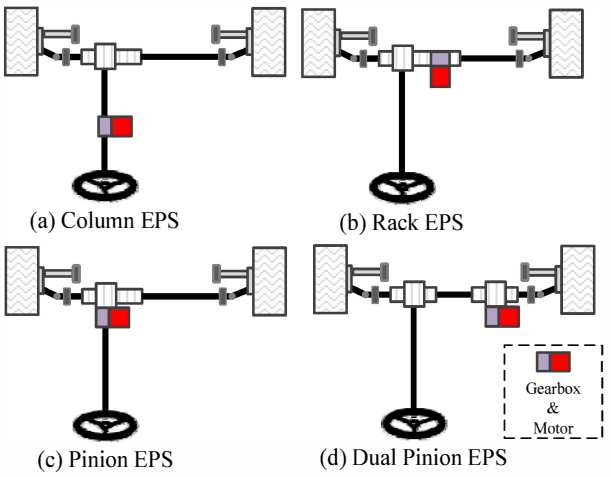

Fig. 1 Classification of EPS systems

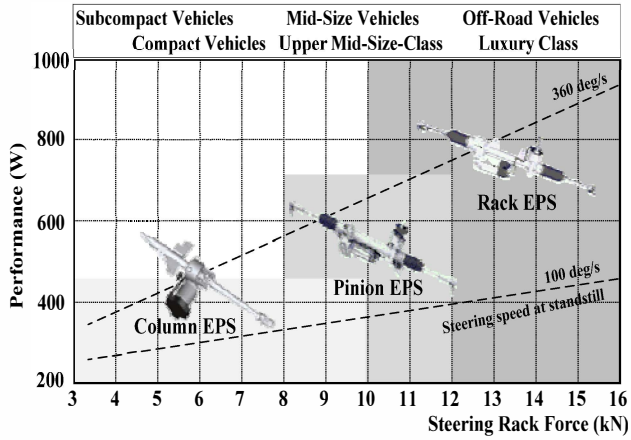

Fig. 2 EPS system application based on vehicle size

2.2 Vehicle model and column EPS model

Fig. 3 shows a schematics diagram of the vehicle lateral dynamics model. A bicycle model is created by lumping the two front and two rear tires into a single front and rear tire, respectively.

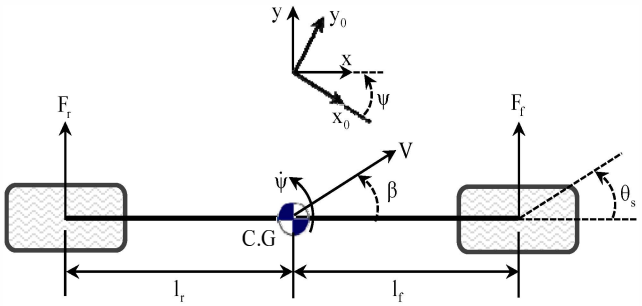

Fig. 3 Bicycle model for vehicle lateral dynamics

As shown in Fig. 3, the pitch and roll dynamic motion is also neglected, and the lateral dynamics of the vehicle can be expressed as follows:

$$mV\left(\dot{\psi}+\dot{\beta}\right)=F_f+F_r \tag{1}$$

$$I_z\ddot{\psi}=l_fF_f+F_rl_r \tag{2}$$

where m is the vehicle mass, V is the vehicle longitudinal velocity, F_f is the front tire force, F_r is the rear tire force, I_z is the equivalent yaw moment inertia, and $\ddot{\psi}$ is the yaw rate angle.

As shown in Fig. 4, the schematic diagram of the column EPS system consists of a steering wheel, torque angle sensor, motor, gearbox, and rack and pinion mechanism. According to Newton's law, the column EPS dynamic equations can be expressed as follows:

$$T_d-k_s\left(\theta_s-\theta_c\right)-B_s\frac{d\theta_s}{dt}=J_s\frac{d^2\theta_s}{dt^2} \tag{3}$$

$$T_e+T_f-B_c\frac{d\theta_c}{dt}+k_s\left(\theta_s-\theta_c\right)-k_r\left(\theta_s-\theta_c\right)=J_c\frac{d^2\theta_c}{dt^2} \tag{4}$$

$$\frac{k_r}{r}\left(\theta_c-\frac{x_r}{r}\right)-F_r-b_r\frac{dx_r}{dt}=m_r\frac{d^2x_r}{dt^2} \tag{5}$$

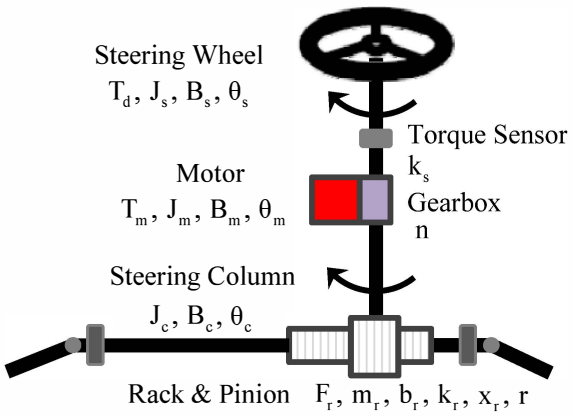

Fig. 4 Schematic diagram of column EPS system

where T_d is the instruction torque on the steering wheel from the driver, J_s is the rotational inertia of the column steering, B_s is the damping coefficient of the column steering wheel angle, and θ_s is the steering wheel angle. T_m is the motor torque, J_m is the rotational inertia of the motor, B_m is the damping coefficient of the motor, and θ_m is the motor angle. J_c is the rotational inertia of the steering column, B_c is the damping coefficient of the steering column, θ_c is the steering column angle, F_r is the alignment force

on the rack from the road wheel, m_r is the mass of the rack, b_r is the damping constant of the rack, k_r is the stiffness between the rack and pinion, x_r is the displacement if the rack, r is the stroke ratio, k_s is the stiffness of the torsion bar, and n is the gearbox gear ratio. Finally, T_e and T_f are the electromagnetic drive and friction torques on the steering column, respectively.

The electromagnetic drive torque on the steering column depends on the motor current, as shown in Eq. (4). Therefore, it is determined by the steering torque sensor (k_s).

$$T_e = k_a k_s (\theta_s - \theta_c) \quad (0 \le k_a \le k_a^{max}) \tag{6}$$

The steering assist gain (k_a) is determined by the road condition (i.e., F_f, F_r) and the vehicle driver's feeling. Therefore, its value is an important turning parameter of the EPS system. The steering assist gain is exponentially decreased by the vehicle velocity. Therefore, the relationship between the steering assist gain (k_a) and vehicle velocity (V) can be expressed as follows:

$$k_a = te^{-kV} \quad (0 \le V \le V^{max}) \tag{7}$$

The EPS assist torque (T_a) depends on the vehicle velocity (V) and driver steering input torque (T_d). In other words, the main inputs of the EPS control algorithm are the vehicle velocity and driver steering input torque. Eqs. (3), (4), and (5) are the steering column, rack column, and motor dynamic equations, respectively, and the EPS assist torque can be expressed as follows:

$$T_a = f(V, T_d) \tag{8}$$

$$T_a = k_s \left(\theta_m - \frac{n}{r} x_r \right) \tag{9}$$

2.3 Advanced Control Strategy for EPS System

As shown in Fig. 5, the proposed advanced control strategy for the EPS motor assist torque (T_m) utilizes three primary inputs: the driver steering input torque (T_d), vehicle velocity (V), and front tire lateral force (F_y^f).

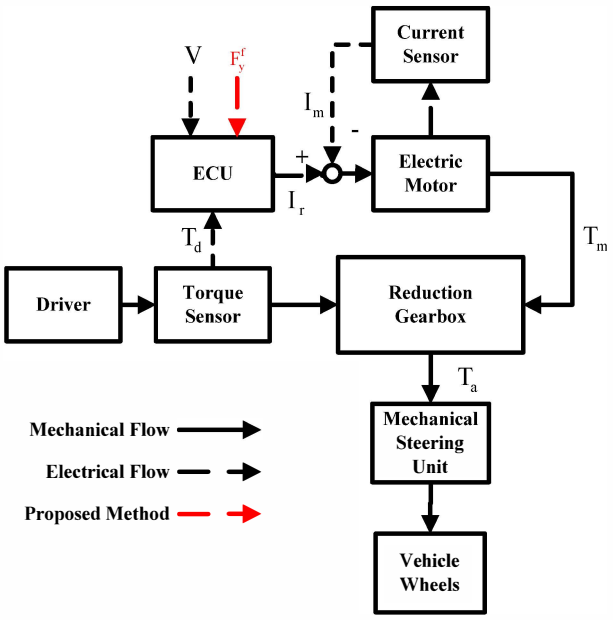

Fig. 5 Block diagram of proposed EPS control

where I_r is the reference current, I_m is the measured motor current, T_d is the driver steering torque, and T_a is the steering assist torque.

The driver steering input torques (T_d) can be detected by a torque sensor, and the vehicle longitudinal velocity (V) can be detected by a vehicle speed sensor (i.e., wheel speed sensor or engine ECU).

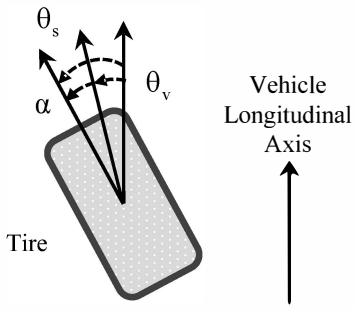

Fig. 6 Tire slip angle

where F_y^f is the front tire lateral force, θ_v is the vehicle velocity vector, and α is the tire slip angle.

The lateral force of the front tires is defined as the relationship between the front left tire lateral force (F_y^{fl}) and the front right tire lateral force (F_y^{fr}), and it can be expressed as follows:

$$F_y^f \triangleq \frac{1}{2}\left(F_y^{fl} + F_y^{fr}\right) \tag{10}$$

$$F_y^f = \frac{ml_r a_y + I_z \ddot{\psi}}{l_f + l_r} = C_f \alpha_f = C_f \left(\theta_s - \beta - \frac{l_f}{V} \dot{\psi} \right) \quad (11)$$

$$\beta = \left(-ma_y + \frac{l_r C_r - l_f C_f}{V} \dot{\psi} + C_f \theta_s \right) \times \frac{1}{C_f + C_r} \quad (12)$$

where F_y^{fl} is the front left tire lateral force, F_v^{fr} is the front right tire lateral force, β is the side slip angle, C_f is the cornering stiffness of the front tires, C_r is the cornering stiffness of the rear tires, and α_f is the sideslip angle of the front tires.

$$T_{ap} = f\left(V, T_d, F_y^f\right) \quad (13)$$

Combining Eqs. (11) and (13), the proposed EPS assist torque (T_{ap}) can be described as follows:

$$T_{ap} = k_p \left(T_d \cdot C_f \left(\theta_s - \beta - \frac{l_f}{V} \dot{\psi} \right) \right) \quad (14)$$

In this paper used to the vehicle mass (m), rotational inertia vehicle mass (I_z), and front/rear tires cornering stiffness (C_f / C_r). According to the above assumption, the steering assist gain (k_p) can be expressed as follows:

$$k_p = t\left(e^{-kV} + e^{kF}\right) \quad \left(0 \le V \le V^{max},\ 0 \le F \le F^{max}\right) \quad (15)$$

The magic tire model is used to represent the vehicle's longitudinal, lateral, and vertical motions. The reference vehicle specifications are listed in Table 1 and Fig. 7.

Table 1 Reference vehicle specifications

Symbol	Quantity	Value
I_z	Moment of vehicle inertia	2,500 (kgm^2)
C_f	Cornering stiffness of the front tire	95,700 (N/rad)
C_r	Cornering stiffness of the rear tire	287,000 (N/rad)
l_f	Distance of C.G from front axle	1,120 (mm)
l_r	Distance of C.G from rear axle	1,530 (mm)
m	Vehicle mass	1,500 (kg)

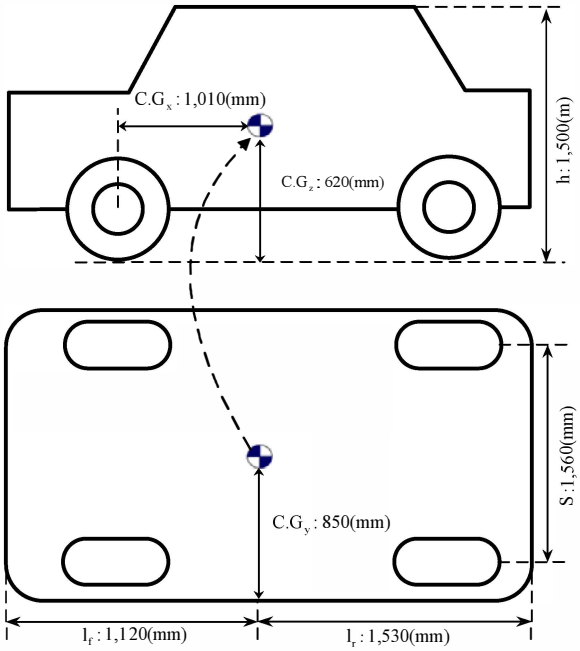

Fig. 7 Vehicle dynamics modeling

3. TEST VALIDATION

3.1 Simulation Test Maneuvers

The developed advanced control strategy for the EPS system is implemented for DLC test maneuvers. The EPS steering assist torque is smaller than that at low velocity in the DLC test maneuver. However, the proposed EPS system assist torque method is verified by the lateral force of the front tires. As listed in Table 2 and Fig. 8, the test was conducted on a 61-m-long roadway with two 3.7-m-wide lanes. The DLC test included entry and exit lanes with a length of 12 m and a side lane with a length of 11m. The simulation was conducted with the EPS system at a vehicle velocity of 80kph.

Table 2 Double lane change parameters

Sec.	Length	Offset	Width
1	12.0(m)	-	$1.1 \times \sigma + 0.25$
2	13.5(m)	-	-
3	11.0(m)	1	$\sigma + 1.0$
4	12.5(m)	-	-
5	12.0(m)	-	$1.3 \times \sigma + 0.25$

* σ : track width

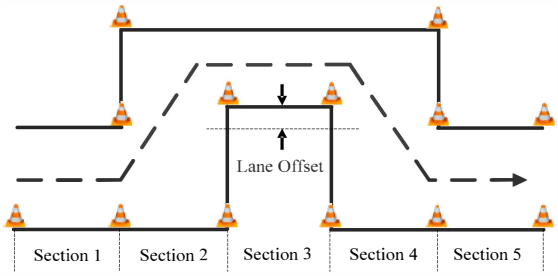

Fig. 8 Double lane change test maneuver

3.2 Test Results

The passenger vehicle DLC test was performed to verify the effectiveness and performance of the proposed EPS assist torque for the applied front tire lateral force. Figs. 9–16 show the results for the lateral force of the tires and steering assist wheel torque. As shown in Fig. 16, the conventional EPS assist torque is approximately -5 ~ 4.5N and the proposed EPS assist torque is -4 ~ 4.4N. Fig 17 shows the performance of advanced EPS implemented on the same vehicle and road friction, and evaluated at diverse velocity conditions. In this velocity range is $5 \leq V < 40$kph low velocity range and $40 \leq V < 80$kph is medium velocity range and $80 \leq V < 120$kph is high velocity range.

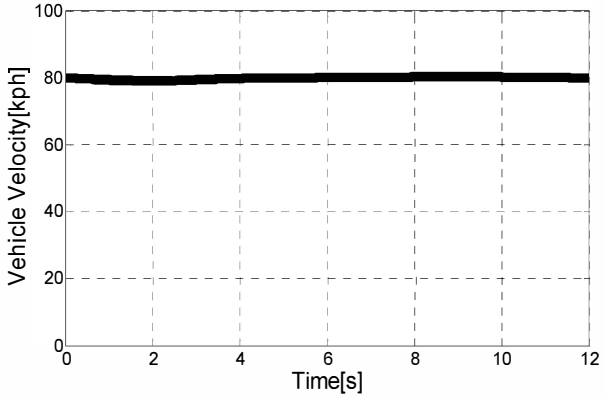

Fig. 9 Vehicle velocity results of DLC test

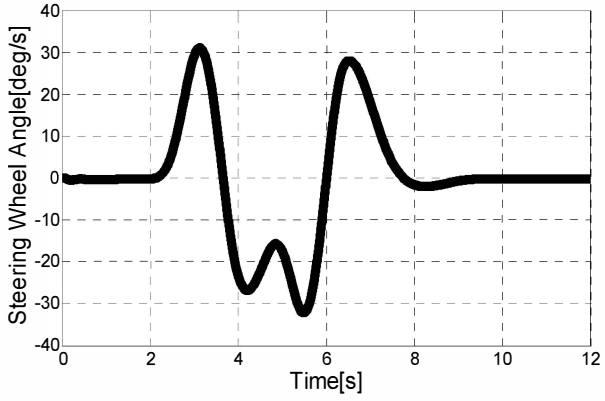

Fig. 10 Steering wheel angle results of DLC test

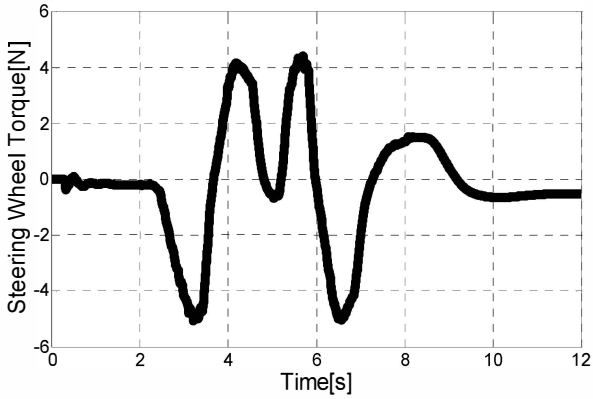

Fig. 11 Steering wheel torque results of DLC test

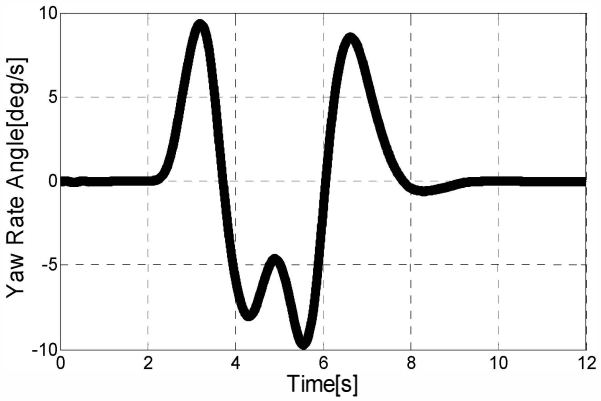

Fig. 12 Yaw rate angle results of DLC test

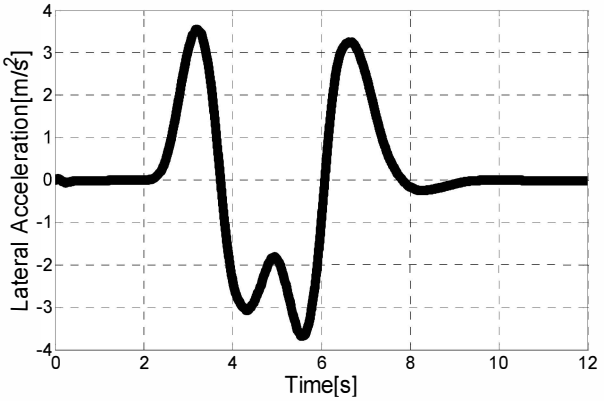

Fig. 13 Lateral acceleration results of DLC test

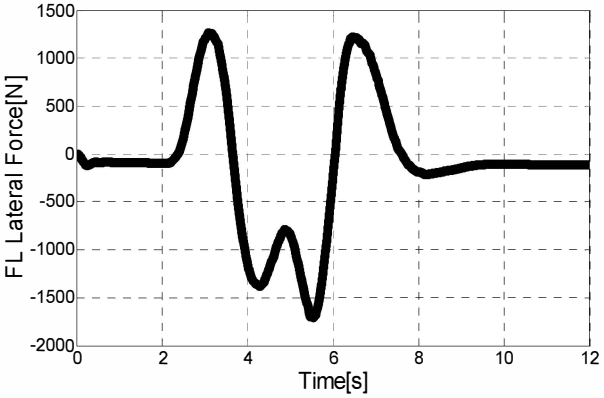

Fig. 14 Front left tire lateral force in DLC test

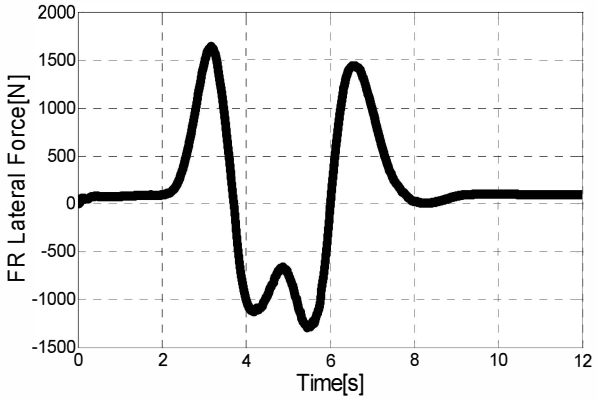

Fig. 15 Front right tire lateral force in DLC test

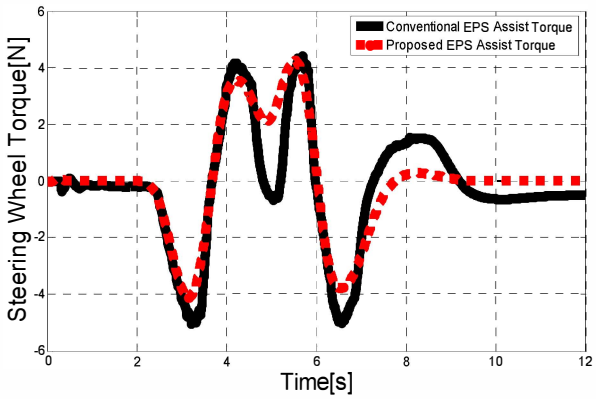

Fig. 16 Proposed steering wheel torque results in DLC test

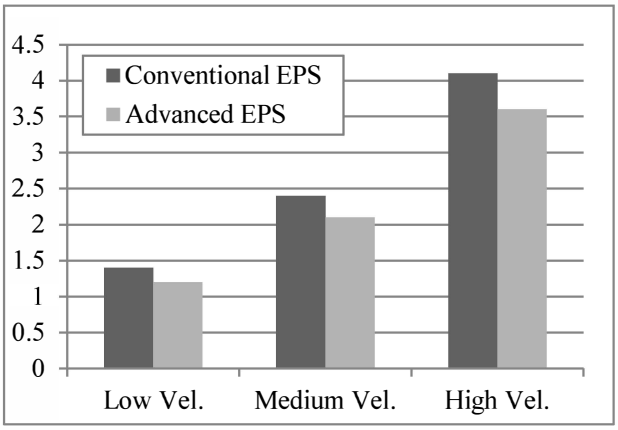

Fig. 17 Average EPS assist torque (N)

4. CONCLUSION

This paper showed how an advanced EPS control strategy was developed and implemented in a simulation test. The proposed assist torque was based on the driver input steering torque, vehicle velocity, and lateral force of the front tires in this study. The simulation test results showed that the proposed EPS assist torque method reduces the assist torque and saves power in the EPS actuator. As Fig 17 shows, the EPS assist torque was reduced compared to that with the conventional EPS control method. In this result, the average EPS assist torque was reduced by about 12% at high and medium velocities. In addition, the average EPS assist was reduced by 14% at the low velocity. Therefore, the proposed EPS assist method should achieve the same performance with less EPA assist torque. The advanced EPS control method should also improve the driver's steering feel characteristic, which is consistent with the lateral force of the tires.

Although it is difficult to directly measure the lateral force of the tires using the current mass production technology for vehicles, this method could be applied using EPS control engineering and sensor improvements to overcome the technical limitation. In future work, sensors will be added to improve the assist torque reduction and driving stability.

REFERENCES

[1] S. Chung, J. M. Kim, J. M. Kim et al, "Development of the Analysis Simulator for EPS Handling Performance Effects by Tire Design Parameter," *KSAE Annual Conference Proceedings*, pp. 889-894, 2013

[2] H. Wi, G. Jo, J. Park, K, Park and J. Lee, "Effect of Type of Power Steering System on Vehicle Fuel Economy," *KSAE Annual Conference Proceedings*, pp. 733-738, 2006

[3] M. Kurishige et al, "A New EPS Control Strategy to Improve Steering Wheel Returnability," *SAE International Paper*, SAE 2000-01-0815, 2000

[4] Z. He, M. Gu, "Dynamic Research on Control Strategy of Electric Power Steering System," *SAE International Paper*, SAE 2012-01-0212, 2012

[5] M. Kurishige, S. Wada, T. Kifuku, N. Inoue, R. Nishiyama and S. Otagaki, "An EPS Control Strategy to Improve Steering Wheel Returnability" *SAE International Paper*, SAE 2000-01-0815, 2000

[6] M. Kurishige et al, "An EPS Control Strategy to Improve Steering Maneuverability on Slippery Roads," *SAE International Paper*, SAE 2002-01-0619, 2002

[7] H. Tanaka et al, "Torque Controlled Active Steer for EPS," *AVEC Paper*, No. 83, 2004

[8] M. Kurishigel, T. Kifuku, N. Inoue, S. Zeniya and S. Otagaki "A Control Strategy to Reduce Steering Torque for Stationary Vehicle Equipped with EPS," *SAE International Paper*, SAE 1999-01-0403, 1999

[9] H. Kim, J. Ryu, H. Choi and H. Kim, "Effects of EPAS(Electric Power Assist Steering) Motor Torque Ripple on Steering Feel and Vehicle Turning Behavior," *KSAE Annual Conference Proceedings*, pp. 801-806, 2005

[10] K. Y. Cho, Y. K. Lee et al, "Torque Ripple Reduction of a PM Synchronous Motor for Electric Power Steering using a Low Resolution Position Sensor," *Journal of Power Electronics. Vol., 10, No. 6,* JPE 10-6-8, 2010

[11] S. Kim, D. Chung, J. Kim and D. Choi, "Improvement of On-center Handling Performance in Electric Power Steering," *KSAE Annual Conference Proceedings*, pp. 405-410, 2002

[12] J. Park, S. Kim, H. Jung et al, "Nonlinear Steering System and Vehicle Model Development for the On-Center Handling Simulation," *KSAE Annual Conference Proceedings*, pp. 27-35, 2003

[13] G. Ruck, "IQPC Advanced Steering Systems, ZF Lenksysteme," 2006